catalysts

MDPI

Article

Real-Time Degradation of Indoor Formaldehyde Released from Actual Particle Board by Heterostructured g-C_3N_4/TiO_2 Photocatalysts under Visible Light

Qing Jin [1], Youlin Xiang [1] and Lu Gan [1,2,*]

[1] College of Materials Science and Engineering, Nanjing Forestry University, Nanjing 210037, China
[2] Jiangsu Co-Innovation Center of Efficient Processing and Utilization of Forest Resources, International Innovation Center for Forest Chemicals and Materials, College of Materials Science and Engineering, Nanjing Forestry University, Nanjing 210037, China
* Correspondence: ganlu@njfu.edu.cn

Abstract: Indoor formaldehyde pollution causes a serious threat to human health since it is uninterruptedly released from wooden furniture. Herein, we prepared a g-C_3N_4-modified TiO_2 composite photocatalyst and coated it on the surface of a commercial artificial particle board with the assistance of melamine formaldehyde adhesive. The g-C_3N_4/ TiO_2 coating was then used to degrade formaldehyde which was released in real-time from the particle board under the irradiation of visible light. The results showed that compared with pure TiO_2, the g-C_3N_4/ TiO_2 composite with a heterojunction structure had a lower band gap energy (~2.6 eV), which could effectively capture luminous energy from the visible light region. Under continuous irradiation, the g-C_3N_4/ TiO_2 photocatalytic coating was capable of degrading more than 50% of formaldehyde constantly released from the particle board. In the meantime, the photocatalytic coating also exhibited promising catalytic stability towards various formaldehyde release speeds, air flow velocities and environmental humidities. The hydroxyl radical and superoxide radical were found to be the predominant active species which triggered formaldehyde degradation. This study provides a feasible and practical approach for the improvement in indoor air quality through photocatalyst surface engineering.

Keywords: photocatalyst; TiO_2; g-C_3N_4; heterostructure; formaldehyde degradation

Citation: Jin, Q.; Xiang, Y.; Gan, L. Real-Time Degradation of Indoor Formaldehyde Released from Actual Particle Board by Heterostructured g-C_3N_4/TiO_2 Photocatalysts under Visible Light. *Catalysts* **2023**, *13*, 238. https://doi.org/10.3390/catal13020238

Academic Editors: Gassan Hodaifa, Rafael Borja and Mha Albqmi

Received: 29 December 2022
Revised: 13 January 2023
Accepted: 17 January 2023
Published: 19 January 2023

1. Introduction

Indoor volatile organic compounds (VOCs) released from wooden furniture have received tremendous attention, and of these formaldehyde (HCHO) is regarded as one of the most frequently released VOCs [1,2]. If HCHO cannot be completely removed, it may cause severe threats to human health, such as nasal tumors and skin cancer [3]. Although many techniques such as ventilation, adsorption, plasma and thermal catalytic oxidation have been conducted to remove HCHO, it is still relatively difficult to find an all-weather approach which can detect the released HCHO in real-time and promptly remove it, since HCHO is continuously volatilized from indoor wooden building materials during daily life [4].

More recently, photocatalytic technology has emerged as a promising means to quickly remove HCHO from indoor air [5]. Under the irradiation of light, HCHO molecules can be effectively oxidized to inorganic H_2O and CO_2 by semiconductor-based photocatalysts [6]. Amongst all applicable photocatalysts, titanium oxide (TiO_2) is the most frequently selected due to high stability, low toxicity and low cost [7]. However, the wide application of TiO_2 still encounters many limitations since it is a UV light-responsive photocatalyst which cannot effectively utilize the energy from the visible light region [8]. The hybridization of other semiconductors, such as ZnO, CdS, SnO2, etc., with TiO_2 can readily improve the photocatalytic activity of TiO_2 through constructing a heterojunction structure, which

can lead to higher charge collection and separation efficiency [9]. Graphitic carbon nitride (g-C_3N_4) is a two-dimensional metal-free n-type semiconductor which has been intensively studied recently as a visible light-responsive photocatalyst. Compared with other metal compound-based photocatalysts, g-C_3N_4 has the merits of a proper band gap energy (~2.7 eV), low toxicity and ease of accessibility [10]. Many studies have shown that g-C_3N_4 can be introduced as a second phase to hybridize with other semiconductors and build heterostructure photocatalysts with highly elevated catalytic capabilities [11]. Therefore, it is possible to prepare a heterostructure composite photocatalyst with high HCHO removal efficiency through integrating g-C_3N_4 with TiO_2.

Another concern when utilizing photocatalysts for indoor HCHO degradation in real living spaces is that most photocatalysts have a powdery form, which cannot be easily attached to wooden materials. Furthermore, most previous studies focusing on the photocatalytic degradation of HCHO mainly investigated HCHO degradation with a fixed concentration of HCHO in air [12]. However, in actual conditions, HCHO is continuously released from wooden furniture and the concentration of HCHO in the air fluctuates [13]. Thus, in this study, g-C_3N_4/TiO_2 composite photocatalysts were prepared and used for real-time degradation of the HCHO released from commercial artificial particle board. The prepared photocatalyst was adhered onto the surface of the board as a photocatalytic coating with the assistance of melamine formaldehyde adhesive. The stability for long-term use of the g-C_3N_4/TiO_2 composite towards continuous HCHO release from the artificial board was studied in detail.

2. Results and Discussion

The morphology of the prepared photocatalysts were observed first in terms of SEM, with the results shown in Figure 1. It was seen from Figure 1a that pure TiO_2 had a nanoparticle appearance. Based on the Scherrer formula, the particle size of TiO_2 was calculated to be ~10 nm. Meanwhile, g-C_3N_4 exhibited a layered structure (Figure 1b). When two components were hybridized, it could be observed that TiO_2 nanoparticles were uniformly anchored on the surface of g-C_3N_4 (Figure 1c). With the increase in g-C_3N_4 content in the composite, a lower amount of TiO_2 nanoparticle aggregations could be seen (Figure 1d) since g-C_3N_4 could provide more surface area.

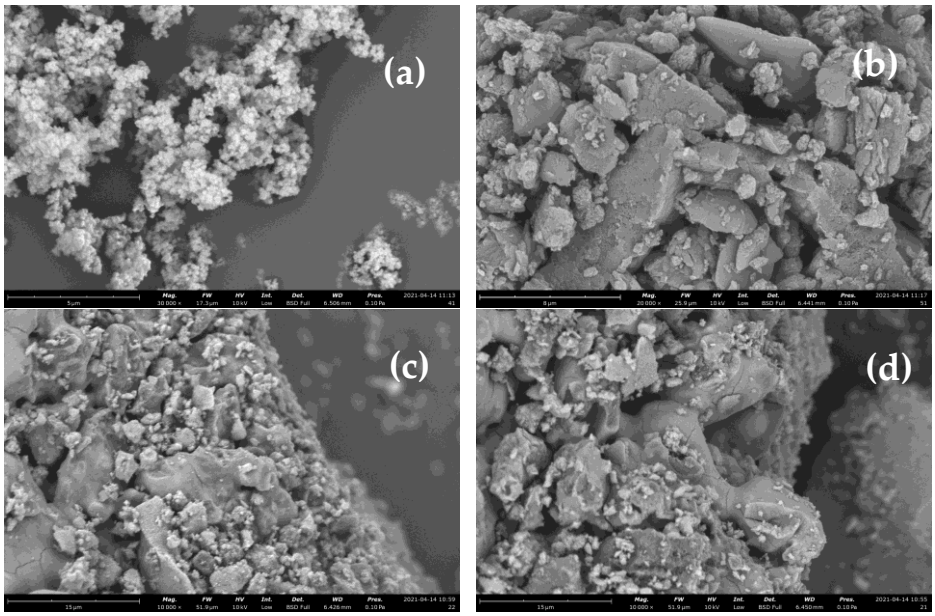

Figure 1. SEM images of (**a**) TiO_2, (**b**) 10-g-C_3N_4/TiO_2, (**c**) 20-g-C_3N_4/TiO_2, (**d**) 30-g-C_3N_4/TiO_2.

The structure of g-C_3N_4/TiO_2 composites was further investigated. Figure 2a shows the XRD patterns of the prepared samples. As illustrated, the prepared TiO_2 exhibited a

typical anatase structure (JCPDS 04-0477) which had characteristic peaks located at 25° (101), 38° (004), 48° (200), 54 (105) and 55° (211) [14]. Based on the Bragg formula, the d-spacing for the (101) lattice plane was calculated to be ~0.35 nm. It was also seen that g-C_3N_4 had two distinct peaks at 13° and 27°, which were indexed to the (100) and (002) lattice planes of its hexagonal graphitic structure (JCPDS 87-1526) [15]. According to the Bragg equation, the d spacing for the (002) lattice plane was calculated to be 0.33 nm, which was close to the interlayer spacing of the graphite crystal. The g-C_3N_4/TiO_2 composites showed integrated patterns in which both characteristic peaks from TiO_2 and g-C_3N_4 could be observed. With the increase in g-C_3N_4 content, the (100) peak of g-C_3N_4 became more apparent, and increased incorporation of g-C_3N_4 did not break the crystalline structure of TiO_2.

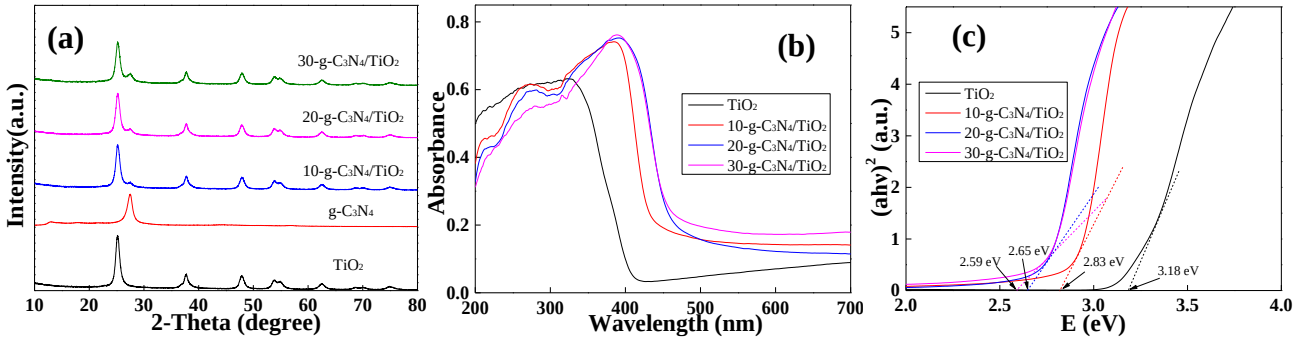

Figure 2. (**a**) XRD patterns, (**b**) DRS spectra and (**c**) corresponding band gap energy of TiO_2 and g-C_3N_4/TiO_2 composites.

The absorbance properties of the prepared photocatalysts were investigated through DRS spectra, with the results shown in Figure 2b. For pristine TiO_2, the absorption edge occurred at a wavelength of lower than 400 nm, indicating that the anatase phase TiO_2 was only responsive to UV light [16]. When g-C_3N_4 was incorporated, the absorption edges of the resulting composites all shifted to the visible light region, indicating that heterostructured g-C_3N_4/TiO_2 could capture visible light to initiate electron/hole separation. The band gap energy (E_g) of the prepared photocatalysts could be further calculated via Tauc plots, with the results shown in Figure 2c. As expected, pristine TiO_2 had an E_g of 3.18 eV, which was in accordance with many previous studies [17]. In the meantime, all the composite photocatalysts had smaller E_g values, in which a higher g-C_3N_4 incorporation amount could lead to narrower E_g. It was noted that the E_g values for 20-g-C_3N_4/TiO_2 (2.65 eV) and 30-g-C_3N_4/TiO_2 (2.59 eV) were both lower than that of pristine g-C_3N_4 (~2.7 eV) [18], indicating that g-C_3N_4 and TiO_2 formed a heterojunction structure which could effectively enhance the light absorption ability of the composite photocatalysts.

The photocatalytic performance of the prepared g-C_3N_4/TiO_2 towards indoor HCHO removal (continuously released from artificial particle board) was then investigated. Figure 3 shows the HCHO degradation capability of the prepared samples. As illustrated in Figure 3a, HCHO was quickly released from the particle board and the adsorption/desorption equilibrium of ~0.64 g/m^3 was reached within 30 min. When the light was off, all the tested boards, coated with different photocatalysts, exhibited a similar HCHO release curve, indicating that each photocatalyst coating barely adsorbed the HCHO in the air. When the UV lamp was on (Figure 3b), the equilibrium concentration of HCHO quickly rose to ~0.78 g/m^3, since UV light could introduce more thermal energy into the reaction chamber which facilitated HCHO release. It was observed that under the irradiation of UV light, HCHO concentration in the air was significantly reduced to a different extent, which was caused by the photocatalytic degradation of HCHO on the coating surface. It was seen that all the g-C_3N_4/TiO_2 composites showed better HCHO degradation performance than pure TiO_2, e.g., the real-time HCHO concentration could be reduced to lower than 0.2 g/m^3 by both 20-g-C_3N_4/TiO_2 and 30-g-C_3N_4/TiO_2. In the meantime, the catalyst

had very promising long-term use stability, as it could unceasingly degrade perpetually released HCHO from the particle boards for more than 24 h. This signified that the high-performance photocatalyst coating on the wooden furniture was a potential and applicable way to lower the concentration of HCHO in the air when the release of HCHO from the wooden furniture theoretically could not be inhibited.

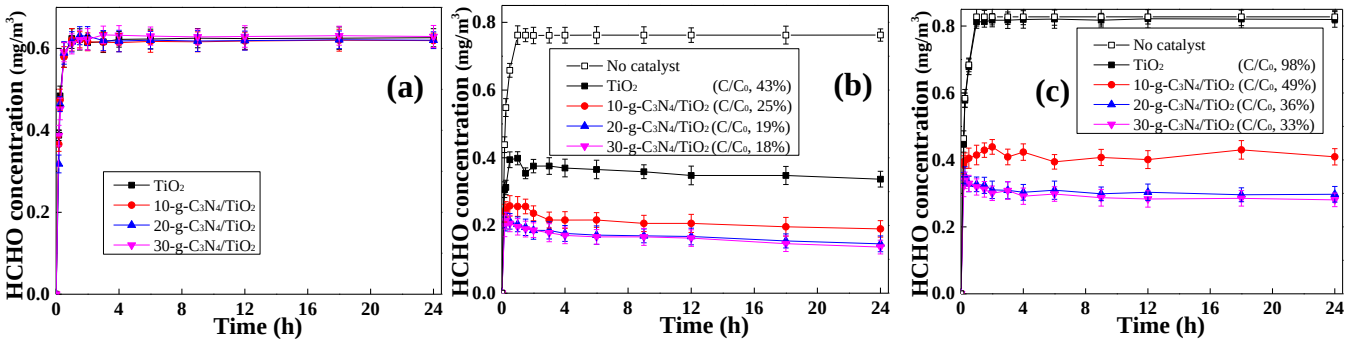

Figure 3. (**a**) Adsorptive removal of HCHO and photocatalytic degradation of HCHO under (**b**) UV light and (**c**) visible light by TiO_2 and g-C_3N_4/TiO_2 composites ($m_{(photocatalyst)}$ = 1 g).

When the light source was changed to a Xe lamp (Figure 3c), the HCHO equilibrium concentration in the reaction box was increased to even higher than 0.80 g/m^3 due to the thermal radiation source nature of the Xe lamp. As anticipated, TiO_2 showed negligible HCHO removal capability since the UV responsible photocatalyst could not effectively generate energy from visible light irradiation [19]. On the contrary, all the composite photocatalysts still exhibited excellent HCHO degradation performance under visible light, with 20-g-C_3N_4/TiO_2 and 30-g-C_3N_4/TiO_2 also presented the optimal efficiency. Specifically, more than 60% of the HCHO could be degraded by these two photocatalyst-based coatings at any time of release. The results demonstrated that compared with TiO_2, g-C_3N_4/TiO_2 was more suitable to be coated on wooden furniture to reduce indoor HCHO concentration since visible light is more than 50% of natural light, whereas UV light is only 5% [20].

The influence of the coating parameters, including the catalyst dosage, of the coating and HCHO concentration on the performance of the composite catalyst was then investigated, with the results shown in Figure 4. In these cases, 20-g-C_3N_4/TiO_2 was selected as the test catalyst due to its high performance. A Xe lamp was used as the light source. As demonstrated in Figure 4a, the performance of 20-g-C_3N_4/TiO_2 did not fluctuate much with changes in its initial dosage in the coating solution, which might because a magnified amount of the catalyst particles could not increase the exposed active sites on the coating surface, and the contact between HCHO and the active sites of 20-g-C_3N_4/TiO_2 was not enhanced as a result, since only surface photocatalyst particles could be irradiated by the incident light and generate active species for HCHO degradation. When the particle board was changed to those with different HCHO releasing rates, it was shown from Figure 4b that the photocatalyst still exhibited high HCHO real-time degradation performance towards all selected panels. Notably, the 20-g-C_3N_4/TiO_2 coating gave the highest HCHO removal efficiency to the board with the highest HCHO releasing rate, which might because more HCHO molecules were in contact with the g-C_3N_4/TiO_2 particles in the fixed volume chamber.

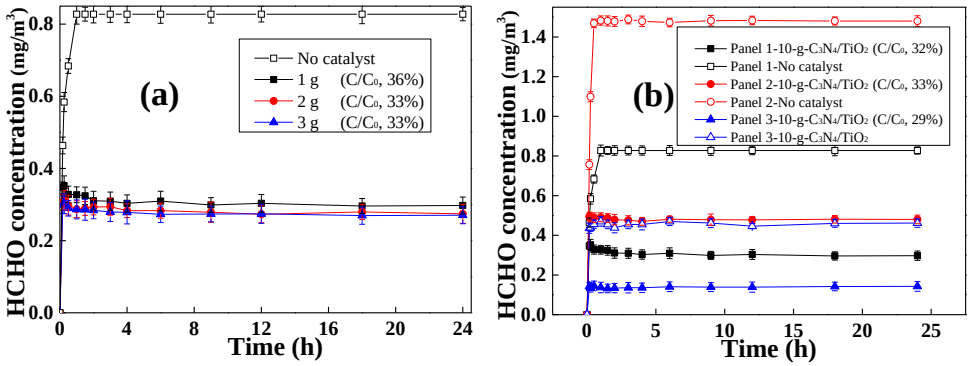

Figure 4. Impact of (**a**) photocatalyst coating amount and (**b**) HCHO release velocity on the photocatalytic performance of 20-g-C_3N_4/TiO_2 composites.

Figure 5 shows the impact of the environmental parameters on the performance of the photocatalyst. The results shown in Figure 5a indicated that by reducing the air flow velocity, the HCHO degradation efficiency was effectively enhanced due to higher contact between the HCHO and 20-g-C_3N_4/TiO_2 at lower air flow velocities. Furthermore, the alteration of environmental air humidity also influenced the HCHO removal rate. It was inferred from Figure 5b that increased humidity could impede the photocatalytic degradation of HCHO. This was because when the water vapor content in the air increased, more water molecules adhered to the 20-g-C_3N_4/TiO_2 coating surface, which hindered the contact rate between the catalyst molecules and pollutant molecules [21]. It was also observed from Figure 5b that a lower humidity also suppressed the performance of the photocatalyst. This indicated that the existence of H_2O in the system was the key for photocatalytic degradation of HCHO. It is generally known that in many cases, when incident light triggers the electron/hole separation in the photocatalyst, the hole in the valence band (VB) needs to react with an ambient hydroxyl ion (OH^-) to form OH to degrade the organic pollutant [22]. Thus, sufficient H_2O molecules existing in the reaction system is necessary to guarantee the conversion from hole to OH [23], which was why a relatively low environmental humidity led to a negative impact to the performance of the composite photocatalyst. However, excessive H_2O molecules could also occupy the active sites on photocatalyst surface when further increasing the humidity to 80%, which also led to a significant decline in the HCHO degradation efficiency.

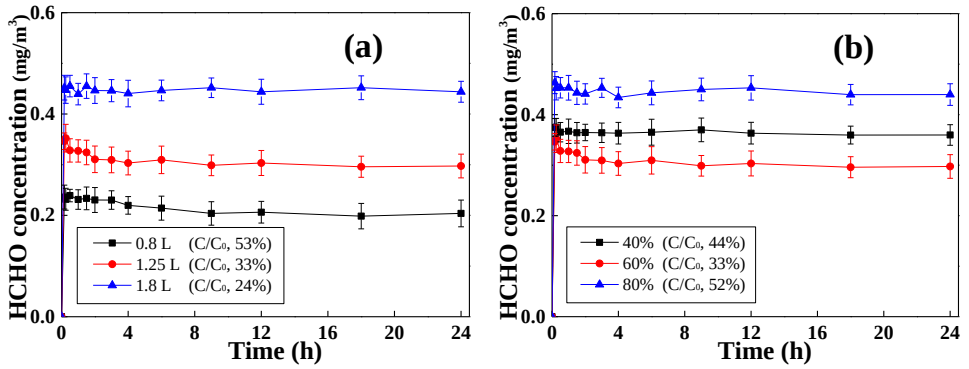

Figure 5. Impact of (**a**) air flow velocity and (**b**) environmental humidity on the photocatalytic performance of 20-g-C_3N_4/TiO_2 composites.

The predominant active species which initiated HCHO degradation was then investigated, with the results shown in Figure 6a. It was clearly seen that both MeOH and t-BQ could inhibit the HCHO removal rate, whereas EDTA could not hinder HCHO degradation. This meant the radicals, including OH and O_2^-, were the main species responsible for the degradation of HCHO [24], where OH and O_2^- were produced from the reaction of holes

in the VB with OH^- and electrons in the conduction band (CB) with ambient oxygen (O_2), respectively. This result could also explain why the performance of 20-g-C_3N_4/TiO_2 was slowed down at low humidity. Figure 6b shows the XRD pattern of used 20-g-C_3N_4/TiO_2 after 24 h of service. It was seen that the used photocatalyst had the same XRD pattern as the freshly made one, indicating a promising long-term use stability.

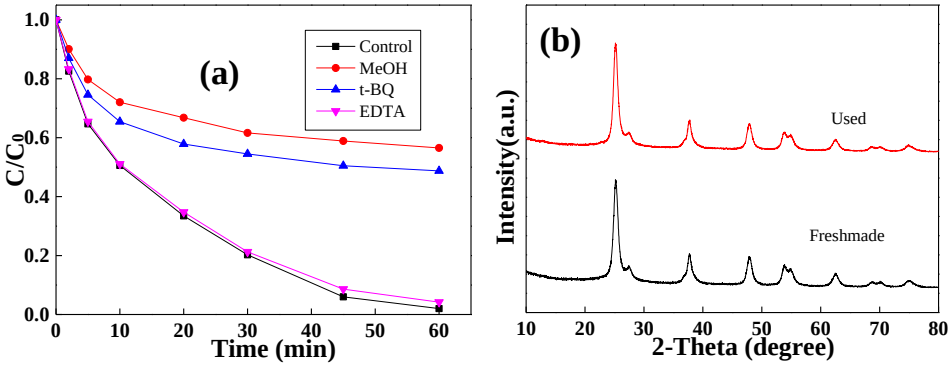

Figure 6. (**a**) HCHO degradation in water with the existence of different scavengers, (**b**) XRD pattern of used 20-g-C_3N_4/TiO_2.

Based on the above overall results, the real-time HCHO degradation process by 20-g-C_3N_4/TiO_2 coating was proposed in Figure 7. In practical conditions, HCHO is incessantly released from indoor wooden furniture, such as the particle board used in this work. If no valid inhibitory approach is conducted, HCHO will quickly occupy indoor spaces. When the photocatalyst coating, which is g-C_3N_4/TiO_2 in this study, is adhered on the furniture surface, the coating can unceasingly degrade HCHO released in real-time under the irradiation of light. Specifically, when a very small amount of g-C_3N_4 was hybridized with TiO_2, a heterojunction-structured composite photocatalyst could be formed. Under such conditions, g-C_3N_4/TiO_2 had a narrower band gap energy with an expanded light adsorption region compared with TiO_2. Therefore, the composite photocatalyst can adsorb visible light for HCHO degradation, where g-C_3N_4 accelerates the separation and suppresses the recombination of the electron/hole pairs. After the electron/hole pairs were produced by visible light irradiation and stabilized by the g-C_3N_4/TiO_2 heterojunction, the excited electrons in the CB quickly reacted with the O_2 in the reaction system to produce O_2^-, and the remaining holes in the VB also reacted with the nearby OH^- to generate OH, both of which caused HCHO degradation in the reaction chamber. As long as the visible light source was on, the constantly released HCHO from the particle board could be removed in real-time with high efficiency by the photocatalyst coating prepared in this study.

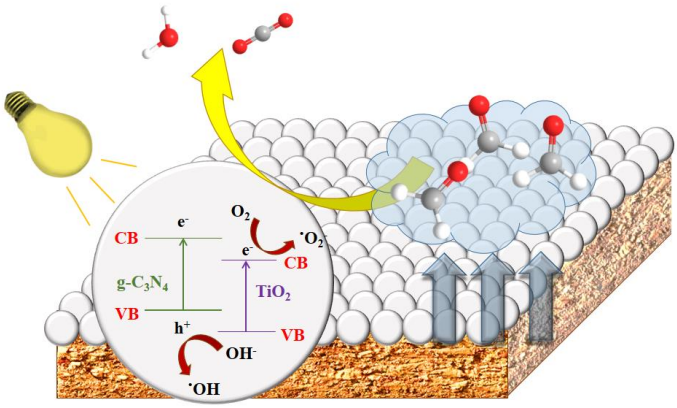

Figure 7. Schematic illustration of real-time HCHO degradation by g-C_3N_4/TiO_2 (Red dot: Oxygen, gray dot: carbon, white dot: hydrogen).

3. Materials and Methods

3.1. Chemical Reagents

Titanium butoxide (TBT, $C_{16}H_{36}O_4Ti$, >99%), melamine ($C_3H_6N_6$, 99%), hexadecyl trimethyl ammonium bromide (CTAB, $C_{19}H_{42}BrN$, 99%) and tert-benzoquinone ($C_6H_4O_2$, 99%) were purchased from Aladdin Co., Ltd. (Shanghai, China). Edetate disodium ($C_{10}H_{14}N_2Na_2O_8 \cdot 2H_2O$, 99–101%) was purchased from Sigma-Aldrich (St. Louis, MI, USA). The artificial particle boards that released different HCHO amounts were provided by Linyi wood factory (Linyi, China). Other chemicals and reagents were of analytical grade and used without further purification.

3.2. Preparation of g-C_3N_4/TiO_2

g-C_3N_4 was prepared by pyrolyzing melamine at 550 °C for 3 h in a muffle furnace. The preparation of g-C_3N_4/TiO_2 composites with different g-C_3N_4 contents was conducted as follows. Firstly, a certain amount of g-C_3N_4 and CTAB (20 mg) were added into 100 mL of ethanol, and the mixture was sonicated for 1 h to obtain a g-C_3N_4 dispersion. Then, TBT (0.5 g) was added and dissolved in the above dispersion, and the mixture transferred into a Teflon-lined stainless-steel autoclave. The autoclave was afterwards heated to 120 °C for 24 h. After the temperature was cooled to room temperature, the photocatalysts named as x-g-C_3N_4/TiO_2 were obtained after the light brown precipitate was separated via centrifuging, washing with H_2O and ethanol twice and drying at 60 °C for 24 h. In the formula, x represents for the mass dosage of g-C_3N_4 in the composites. For comparison, pure TiO_2 was also prepared following a similar procedure without the introduction of g-C_3N_4.

3.3. Characterization and Analytical Methods

The morphology of the prepared samples was determined by scanning electron microscopy (SEM, JEOL SEM 6490, Tokyo, Japan). The X-ray diffraction spectra (XRD) were recorded by a Rigaku Smartlab XRD instrument. The diffuse reflectance spectra (DRS) were conducted by a PerkinElmer Lambda 950 UV/Vis/NIR spectrophotometer.

3.4. Real-Time HCHO Degradation Process

The photocatalytic system for HCHO degradation used in this study is shown schematically in Figure 8. A 50 × 50 × 30 m^3 glass box, equipped with an air inlet pump and a HCHO sensor, was used as the reaction chamber. The glass (with an area of 20 × 20 cm^2) on the top of the chamber was changed to quartz glass for the passage of light. UV light and visible light were both introduced as the light source, in which a 250 W UV lamp was used as the UV light source and a 300 W Xe lamp equipped with a 420 nm cut-off filter was used as the visible light source. All particle boards, with a thickness of 1.5 cm, were cut into 10 × 10 cm^2 rectangular shapes. The particle board was first brushed with a layer of melamine formaldehyde adhesive. Afterwards, 10 mL, 20 mL or 30 mL of the photocatalyst suspension with a concentration of 100 g/L was coated onto the surface of the particle board using a spin-coater at 2000 rpm. After being air-dried for 24 h, the photocatalyst-coated particle board was placed on a lifting table in the glass box, with the distance between the particle board and light source fixed at 18 cm. At the same time, the lamp was turned on to initiate the photocatalytic process, and the HCHO sensor (Dart 2-FE5, Exeter EX4 3AZ, UK) recorded the real-time HCHO concentration in the chamber. The humidity of the reaction chamber was tuned by a commercial mini humidifier. The humidity of the reaction chamber for photocatalytic tests was set at ~60% if not otherwise stated.

The predominant active species generated by g-C_3N_4/TiO_2 for HCHO degradation was identified in aqueous solution by the introduction of different scavengers, in which a Xe lamp was introduced as the light source. Typically, 50 mg of the photocatalyst was added into a 50 mL HCHO solution (10 mg/L) containing 10 mM of methanol (MeOH), tert-benzoquinone (t-BQ) or edetate disodium (EDTA), which were used to trap hydroxyl radicals (OH), superoxide radicals (O_2^-) and holes (h), respectively. After the Xe lamp was turned on, approximately 2 mL of solution was withdrawn from the reaction solution at

predetermined intervals and centrifuged to separate the solid. The concentration of HCHO was quantified using gas chromatography (Agilent 7890A, Agilent, Santa Clara, CA, USA).

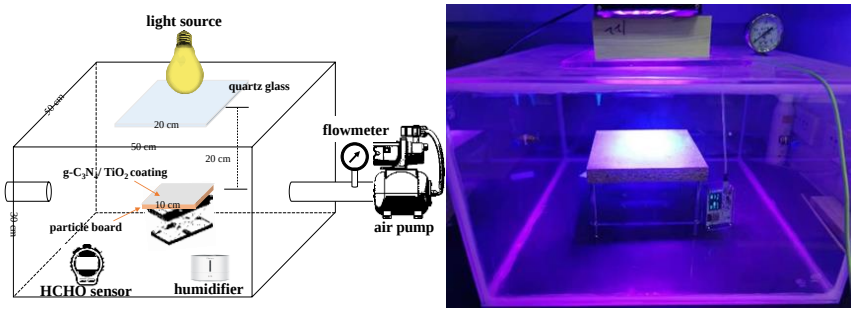

Figure 8. Photocatalytic system for real-time degradation of HCHO released from artificial particle board.

4. Conclusions

To conclude, g-C_3N_4 was modified with TiO_2 to construct composite photocatalysts with a heterojunction structure. The prepared g-C_3N_4/TiO_2 was coated onto the surface of artificial particle board and used for HCHO degradation as it was released in real-time from the particle board under the irradiation of visible light. The prepared g-C_3N_4/TiO_2 exhibited high visible light energy adsorption efficiency since the two components formed an effective heterojunction structure. The g-C_3N_4/TiO_2 coating could unceasingly degrade HCHO which was continuously released from the particle board. The photocatalyst coating also exhibited promising stability and adaptability. The heterostructured g-C_3N_4/TiO_2 prepared in this study can be used for practical indoor air purification.

Author Contributions: Investigation, writing—original draft preparation, Q.J.; methodology, investigation, data curation, Y.X.; conceptualization, writing—review and editing, funding acquisition, L.G. All authors have read and agreed to the published version of the manuscript.

Funding: This research was funded by the Natural Science Foundation of Jiangsu Province, China (BK20201385).

Data Availability Statement: Data are available upon request.

Conflicts of Interest: The authors declare no conflict of interest.

References

1. Chen, J.; Guo, X.; Lang, L.; Yin, X.; Wang, A.; Rui, Z. Multifunctional z-scheme Cu_xO/Ag/$SrTiO_3$ heterojunction for photothermocatalytic vocs degradation and antibiosis. *Appl. Surf. Sci.* **2022**, 153275. [CrossRef]
2. Zhao, Z.Y.; Sun, S.J.; Wu, D.; Zhang, M.; Huang, C.X.; Umemura, K.; Yong, Q. Synthesis and characterization of sucrose and ammonium dihydrogen phosphate (sadp) adhesive for plywood. *Polymers* **2019**, *11*, 16. [CrossRef] [PubMed]
3. Zhang, G.; Sun, Z.; Duan, Y.; Ma, R.; Zheng, S. Synthesis of nano-TiO_2/diatomite composite and its photocatalytic degradation of gaseous formaldehyde. *Appl. Surf. Sci.* **2017**, *412*, 105–112. [CrossRef]
4. Salthammer, T. Formaldehyde sources, formaldehyde concentrations and air exchange rates in european housings. *Build. Environ.* **2019**, *150*, 219–232. [CrossRef]
5. Wang, X.; Hong, S.; Lian, H.; Zhan, X.; Cheng, M.; Huang, Z.; Manzo, M.; Cai, L.; Nadda, A.; Le, Q.V.; et al. Photocatalytic degradation of surface-coated tourmaline-titanium dioxide for self-cleaning of formaldehyde emitted from furniture. *J. Hazard. Mater.* **2021**, *420*, 126565. [CrossRef] [PubMed]
6. Qin, Y.; Wang, Z.; Jiang, J.; Xing, L.; Wu, K. One-step fabrication of TiO_2/Ti foil annular photoreactor for photocatalytic degradation of formaldehyde. *Chem. Eng. J.* **2020**, *394*, 124917. [CrossRef]
7. Li, X.; Li, H.; Huang, Y.; Cao, J.; Huang, T.; Li, R.; Zhang, Q.; Lee, S.-c.; Ho, W. Exploring the photocatalytic conversion mechanism of gaseous formaldehyde degradation on TiO_2–x-Ov surface. *J. Hazard. Mater.* **2022**, *424*, 127217. [CrossRef]
8. Xu, L.; Meng, L.; Zhang, X.; Mei, X.; Guo, X.; Li, W.; Wang, P.; Gan, L. Promoting Fe^{3+}/Fe^{2+} cycling under visible light by synergistic interactions between P25 and small amount of fenton reagents. *J. Hazard. Mater.* **2019**, *379*, 120795. [CrossRef]
9. Li, D.; Li, R.; Zeng, F.; Yan, W.; Deng, M.; Cai, S. The photoexcited electron transfer and photocatalytic mechanism of g-C_3N_4/TiO_2 heterojunctions: Time-domain ab initio analysis. *Appl. Surf. Sci.* **2023**, *614*, 156104. [CrossRef]

10. Xu, L.; Qi, L.; Han, Y.; Lu, W.; Han, J.; Qiao, W.; Mei, X.; Pan, Y.; Song, K.; Ling, C.; et al. Improvement of Fe^{2+}/peroxymonosulfate oxidation of organic pollutants by promoting Fe^{2+} regeneration with visible light driven g-C_3N_4 photocatalysis. *Chem. Eng. J.* **2022**, *430*, 132828. [CrossRef]
11. Li, Y.; Zhou, M.; Cheng, B.; Shao, Y. Recent advances in g-C_3N_4-based heterojunction photocatalysts. *J. Mater. Sci. Technol.* **2020**, *56*, 1–17. [CrossRef]
12. Wu, C. Facile one-step synthesis of n-doped ZnO micropolyhedrons for efficient photocatalytic degradation of formaldehyde under visible-light irradiation. *Appl. Surf. Sci.* **2014**, *319*, 237–243. [CrossRef]
13. He, Z.; Xiong, J.; Kumagai, K.; Chen, W. An improved mechanism-based model for predicting the long-term formaldehyde emissions from composite wood products with exposed edges and seams. *Environ. Int.* **2019**, *132*, 105086. [CrossRef] [PubMed]
14. Manisha; Kumar, V.; Sharma, D.K. Fabrication of dimensional hydrophilic TiO_2 nanostructured surfaces by hydrothermal method. *Mater. Today Proc.* **2021**, *46*, 2171–2174.
15. Jiang, M.; Zou, Y.; Xu, F.; Sun, L.; Hu, Z.; Yu, S.; Zhang, J.; Xiang, C. Synthesis of g-C_3N_4/Fe_3O_4/MoS_2 composites for efficient hydrogen evolution reaction. *J. Alloys Compd.* **2022**, *906*, 164265. [CrossRef]
16. Janus, M.; Choina, J.; Morawski, A.W. Azo dyes decomposition on new nitrogen-modified anatase TiO_2 with high adsorptivity. *J. Hazard. Mater.* **2009**, *166*, 1–5. [CrossRef]
17. Bouzourâa, M.B.; Battie, Y.; En Naciri, A.; Araiedh, F.; Ducos, F.; Chaoui, N. $N2^+$ ion bombardment effect on the band gap of anatase TiO_2 ultrathin films. *Opt. Mater.* **2019**, *88*, 282–288. [CrossRef]
18. Che, H.; Li, C.; Zhou, P.; Liu, C.; Dong, H.; Li, C. Band structure engineering and efficient injection rich-π-electrons into ultrathin g- C_3N_4 for boosting photocatalytic H_2-production. *Appl. Surf. Sci.* **2020**, *505*, 144564. [CrossRef]
19. Khan, T.T.; Bari, G.A.R.; Kang, H.-J.; Lee, T.-G.; Park, J.-W.; Hwang, H.J.; Hossain, S.M.; Mun, J.S.; Suzuki, N.; Fujishima, A. Synthesis of n-doped TiO_2 for efficient photocatalytic degradation of atmospheric NOx. *Catalysts* **2021**, *11*, 109. [CrossRef]
20. Kumar, S.G.; Devi, L.G. Review on modified TiO_2 photocatalysis under UV/visible light: Selected results and related mechanisms on interfacial charge carrier transfer dynamics. *J. Phys. Chem. A* **2011**, *115*, 13211–13241. [CrossRef]
21. Li, Q.; Zhang, S.; Xia, W.; Jiang, X.; Huang, Z.; Wu, X.; Zhao, H.; Yuan, C.; Shen, H.; Jing, G. Surface design of g- C_3N_4 quantum dot-decorated TiO_2(001) to enhance the photodegradation of indoor formaldehyde by experimental and theoretical investigation. *Ecotox. Environ. Saf.* **2022**, *234*, 113411. [CrossRef] [PubMed]
22. Li, M.; Song, C.; Wu, Y.; Wang, M.; Pan, Z.; Sun, Y.; Meng, L.; Han, S.; Xu, L.; Gan, L. Novel z-scheme visible-light photocatalyst based on $CoFe_2O_4$/BiOBr/graphene composites for organic dye degradation and Cr(VI) reduction. *Appl. Surf. Sci.* **2019**, *478*, 744–753. [CrossRef]
23. Li, X.; Jia, Y.; Zhou, M.; Ding, L.; Su, X.; Sun, J. Degradation of diclofenac sodium by pre-magnetization Fe^0/persulfate system: Efficiency and degradation pathway study. *Water Air Soil Pollut.* **2020**, *231*, 311. [CrossRef]
24. Li, X.; Qin, Y.; Song, H.; Zou, W.; Cao, Z.; Ding, L.; Pan, Y.; Zhou, M. Efficient removal of bisphenol a by a novel biochar-based Fe/C granule via persulfate activation: Performance, mechanism, and toxicity assessment. *Process Saf. Environ.* **2023**, *169*, 48–60. [CrossRef]